AAPS PharmSciTech, Vol. 15, No. 6, December 2014 (© 2014)
DOI: 10.1208/s12249-014-0192-x

Research Article

Effect of Arginine on Pre-nucleus Stage of Interferon Beta-1b Aggregation

Ahmad Fazeli,[1] Mohadeseh Haji-Abdolvahab,[2] Seyed Abbas Shojaosadati,[1,6] Huub Schellekens,[2] Khosro Khalifeh,[4] Ali Akbar Moosavi-Movahedi,[5] and Mohammad Reza Fazeli[3]

Received 14 April 2014; accepted 29 July 2014; published online 21 August 2014

Abstract. Understanding the mechanism of aggregation of a therapeutic protein would not only ease the manufacturing processing but could also lead to a more stable finished product. Aggregation of recombinant interferon (IFNβ-1b) was studied by heating, oxidizing, or seeding of unformulated monomeric solution. The formation of aggregates was monitored by dynamic light scattering (DLS) and UV spectroscopy. The autocatalytic monomer loss model was used to fit the data on aggregation rates. The influence of pre-nucleation on aggregation step was demonstrated by inducing the liquid samples containing a monomer form of folded IFNβ-1b by heat and also an oxidizing agent. Results tend to suggest that the nucleus includes a single protein molecule which has been probably deformed. Seeding tests showed that aggregation of IFNβ-1b was probably initiated when 1.0% (*w*/*w*) of monomers converted to nucleus form. Chemiluminescence spectroscopy analysis of the sample indicated the generation of 3.0 μM of hydrogen peroxide (H_2O_2) during nucleation stage of IFNβ-1b aggregation. Arginine with a concentration of 200 mM was sufficient to suppress aggregation of IFNβ-1b by decreasing the rate of pre-nucleation step. We proposed the formation of pre-nucleus structures prior to nucleation as the mechanism of aggregation of IFNβ-1b. Furthermore, we have showed the positive anti-aggregation effect of arginine on pre-nucleation step.

KEY WORDS: aggregation; arginine; interferon beta-1b; mechanism; pre-nucleus.

INTRODUCTION

Recombinant interferon beta (hereafter IFNβ) is a therapeutic protein used to treat the relapsing-remitting and secondary-progressive forms of multiple sclerosis (MS). The non-glycosylated IFNβ-1b (Betaseron®) was the first IFNβ product approved by FDA in 1994 (1). IFNβ-1a (Avonex®) followed in 1996 in the market. The glycosylated IFNβ-1a is produced in CHO cells and has the identical amino acid sequences of natural human IFNβ (2). The non-glycosylated IFNβ-1b has an apparent molecular weight of 18.5 kDa. It is produced in *Escherichia coli* cells, and Cys-17 is mutated to Ser17 to reduce misfolding and/or aggregation during the refolding process (3). Approximately, 60% of the commercially formulated IFNβ-1b protein consists of large, soluble aggregates with an apparent molecular weight of over 600 kDa (3,4). In patients using formulated IFNβ protein, aggregates are a cause of neutralizing antibodies (NAbs) (1,5). The therapeutic effect of IFNβ is influenced by the formation of binding antibodies (BAbs) and NAbs with negative impact on its bioactivity (4). Therefore, aggregation is of great concern affecting the biological activity of IFNβs.

Oxidation of therapeutic proteins could occur during formulation, fill-finish, freeze-drying, or storage (4–7). It is also believed that reactive oxygen species (ROS) have the potential to induce significant biological damages by oxidizing proteins (7). Although aggregate formation looks to be protein specific, there is some evidence to suggest the effect of monomer oxidation (4,7,8). Van Beers *et al.* have showed the effect of protein oxidation on increasing susceptibility to aggregation of IFNβ-1b (5). Also, Chi *et al.* have presented an oxidized form of monomer of α-synuclein as pre-nucleus specie which is prone to aggregation (9). They have also proposed the importance of a similar pathway for other therapeutic proteins undergoing rate-limiting nucleation. Nevertheless, there is no published report directly referencing this phenomenon in the literature.

In native aggregation, a protein undergoes aggregate formation with no effect on its conformation. On the other hand, in nonnative aggregations, the conformation of native molecule changes to an intermediate structure prior to oligomer formation, which is called reactive monomer (10) or aggregation-prone monomer (11). The later mechanism is usually seen in therapeutic proteins.

Cosolvents (or excipients) are widely used in therapeutic protein manufacturing processes and formulations to modify

[1] Biotechnology Group, Department of Chemical Engineering, Tarbiat Modares University, Tehran, Iran.
[2] Departments of Pharmaceutical Sciences and Innovation Studies, Utrecht University, Utrecht, The Netherlands.
[3] Department of Biology, Faculty of Sciences, University of Zanjan, Zanjan, Iran.
[4] Institute of Biochemistry and Biophysics, University of Tehran, Tehran, Iran.
[5] Department of Drug & Food Control, Faculty of Pharmacy and Pharmaceutical Quality Assurance Research Center, Tehran University of Medical Sciences, Tehran, Iran.
[6] To whom correspondence should be addressed. (e-mail: shoja_sa@modares.ac.ir)

the protein's solution behavior (12,13). They can affect solubility and stability of proteins in monomer conformation. Arginine is used to improve refolding yield, due to its ability to suppress protein monomer-monomer interaction and aggregate formation (12–15). There are two main hypotheses for the effect of arginine on monomer stability of proteins. Tsumoto *et al.* suggest the interactions between the guanidine group of arginine and tryptophan side chains of protein surface responsible for anti-aggregation effect of arginine (12–14,16). Instead, Shukla and Trout propose the "gap effect" theory and the concept of "neutral crowders" (17). Arginine is proposed as a neutral crowder who does not affect the free energy of unfolding and is neutral but crowds out the protein-protein interactions due to its larger size as compared to water molecules (18).

Understanding the mechanism of aggregation is an important task in manufacturing and developing formulation of IFNβ-1b. Among different mechanisms and models, the nucleation is a frequent step proposed for aggregation of proteins (19). In order to study the effect of nucleation step through aggregate formation of IFNβ-1b, we tried using the autocatalytic model (19,20). This model holds kinetic physical meanings for nucleation, monomer loss, and fibril growth steps during aggregation (20). The model was assessed by Morris *et al.* through literature data (19). It assumes the aggregation as a process from the monomer to the final aggregate form as two reaction pathways:

$$M \xrightarrow{k_1} A$$
$$M + A \xrightarrow{k_2} 2A$$

In these pathways, monomer of M converts to aggregate form of A, irreversibly, and then A catalyzes the formation of another A from M, where k_1 and k_2 are the rate constants for the first and second reactions. Therefore, the modeling equations are

$$\begin{cases} \dfrac{d[M]}{d[t]} = -k_1[M] - k_2[A][M] \\ \dfrac{d[A]}{d[t]} = k_1[M] + k_2[A][M] \end{cases} \quad (1)$$

Morris *et al.* have assumed that the aggregation consists of two steps: an initial slow continuous nucleation followed by a typically fast autocatalytic surface growth, by considering A as a pre-catalytic form of protein. It is assumed that for an initial monomer concentration of $[M_0]$, there is no aggregate at $t=0$ ($[A_0]=0$), while for a seeded solution, $[A_0]\neq 0$. Although the autocatalytic model has some limitations such as condensing many steps into two pseudo-elementary steps, it is able to deconvolute the average nucleation rate constant from average growth rate constant (19).

In this study, the suppressing effect of arginine on aggregation steps of IFNβ-1b was inspected. This could help us in developing new formulations in the near future. Monomer samples of IFNβ-1b were induced by heating and hydrogen peroxide (H_2O_2) oxidizing to study the kinetics of aggregation. The mechanism and the effect of the nucleation step during aggregation of IFNβ-1b were considered by the autocatalytic model. Also, the significance of pre-nucleus species and generation of ROS were analyzed.

MATERIALS AND METHODS

Materials

The recombinant *E. coli* strain BL21-(DE3) harboring interferon beta-1b gene was obtained from Zistdaru Danesh Ltd. (Tehran, Iran). Native recombinant IFNβ-1b was refolded as fully described in our previous works (21). A desalting Sephadex G-25 chromatography equilibrated with 1 mM sodium hydroxide pH=11 was performed to clean IFNβ-1b from any additives in solution. All other reagents were of analytical grade and purchased from well-known companies. IFNβ-1b protein solution was in sodium hydroxide buffer in all experiments.

Refolding Process

Fed-batch cultivation of recombinant *E. coli* was used to express IFNβ-1b. Inclusion bodies containing IFNβ-1b were isolated and solubilized prior to refolding process. The refolding was carried out in a fed-batch mode by feeding the unfolded IFNβ-1b into a 1-l double jacket reactor as described before (21).

Inducing Aggregation

Heating a solution containing monomer protein is a standard procedure to induce and speed up aggregate formation (9). Hydrophobic interaction is entropy dependent; thus, an increase in the temperature of the system results in aggregation due to intramolecular interactions between monomer proteins (22,23). In order to study the kinetics of aggregation, IFNβ-1b samples with a concentration of 1.4 mg ml^{-1} were incubated at different temperatures of 4, 25, 37, and 70°C or oxidized by H_2O_2 at different concentrations of 0.3, 0.6, and 3.0% (*v*/*v*) (6).

Reversed Phase HPLC

The oxidation of IFNβ-1b proteins was analyzed by reversed phase liquid chromatography and C4 column (Vydac 214T P54) on a HPLC system (Young Lin Instrument) as mentioned before (21). A linear acetonitrile-water gradient with 1% (*v*/*v*) TA at a flow rate of 1 ml min^{-1} was used to elute the samples. The retention time of IFNβ-1b was determined by injection of a standard IFNβ-1b sample into the column. For detection of oxidized protein, a standard IFNβ-1b sample was mixed in 0.5 and 1% *v*/*v* of H_2O_2 as fully described before (21).

Size-Exclusion Ultra-performance Liquid Chromatography

A Waters ACQUITY UPLC system (Waters, Milford, MA, USA) was applied for sample analysis. Samples (7.5 μl, 1 mg/ml) were loaded onto Waters ACQUITY BEH450 SEC (150 mm×4.6 mm, 2.5 μm) UPLC column. Detection took place with a TUV detector (Waters, Milford, MA, USA) at a wavelength of 280 nm and a FLR detector (Waters, Milford, MA, USA) at an excitation of 295 nm and an emission of 340 nm. BEH450 SEC protein standard mix (Waters, Milford, MA, USA) was used to acquire a calibration curve. Prior to measurement, samples were filtered through a 0.2-μm filter

(GE Healthcare, Buckinghamshire, UK) and a flow rate of 0.25 ml/min with total run time of 14 min was operated. Data were collected and analyzed by Empower Software 2.

Aggregate Detection

UV Spectroscopy

Protein concentration was estimated by an optical density (OD) at 280 nm and an extinction coefficient of 1.575 ml mg^{-1} cm^{-1}. The aggregate form of proteins can be observed as an increase in OD at 360 nm and decrease in ratio of $OD_{280\ nm}$/$OD_{260\ nm}$ as presented in the literature (4,5). Turbidity in protein solutions results in the perception of turbidity and scattering at 360 nm, while proteins absorb light at 280 nm due to aromatic groups of amino acids (22). A decrease in the ratio of $OD_{280\ nm}/OD_{260\ nm}$ is a sign of monomer protein aggregation in IFNβ-1b solutions (4,23).

UV absorbance was measured at 25°C in quartz cuvettes with a path length of 1 cm using an Agilent 8453 UV/VIS spectrophotometer. Each sample was centrifuged at 20,000*g*, and the supernatant was collected for analysis. The OD of the supernatant at 280 and 360 nm was measured, and the loss of monomers for each sample was calculated by converting absorbance data to concentration, via van Beer's law and IFNβ-1b extinction coefficient. IFNβ-1b aggregation type was identified by addition of 0.1% of sodium dodecyl sulfate (SDS) to the aggregate samples and mixing for 1 min at room temperature (5). Then, the OD of the samples was read at 280 and 360 nm to detect the concentration of monomers and any aggregate.

Dynamic Light Scattering

Aggregation of IFNβ-1b (1.4 mg ml^{-1}) was analyzed by dynamic light scattering (DLS) to obtain an average diameter of the particles (Z_{ave}) and their polydispersity index (PDI) before and during incubation at 37°C for 1 week. Samples were analyzed with a Malvern CGS-3 Zetasizer and a Dispersion Technology Software version 4.20 at 25°C.

Aggregation Kinetic Calculations

The autocatalytic model was used to study the importance of nucleus formation during aggregation of IFNβ-1b. Kinetic parameters were determined by fitting Eq. 1 on experimental data.

Critical Nucleus Determination

Chen *et al.* approach was used to estimate the number of monomers in the nucleus (known as the critical nucleus) (24). According to this approach, at early times of aggregation, we have

$$[A] = \frac{1}{2}k'[A_0]^2t^2 \tag{2}$$

A plot of $[A]$ *vs.* t^2 gives a linear line with a given slope of α. The value of α was calculated by considering different initial concentrations of 0.6, 1.0, and 1.4 mg ml^{-1} for $[A_0]$. The critical nucleus was determined by the slope of a $\log(-\alpha)$ *vs.* $\log([A_0])$ plot as fully described in the literature (24). The slope=n^*+2, and the intercept=log ($k'/2$), where n^* is the number of monomers in the nucleus and k' is rate constant of aggregation.

Chemiluminescence Spectroscopy

Chemiluminescence method was used to determine the level of H_2O_2 or other ROS in solution as described in the literature (25). In this method, an emitted light is measured upon producing H_2O_2 in a luminol alkaline solution. Each aggregate sample of 1.4 mg ml^{-1} of IFNβ-1b was analyzed by chemiluminescence method with two repeats.

Antiviral Activity

Human lung carcinoma (A549) cell line and encephalomyocarditis virus (EMCV) were used to estimate the antiviral activity of IFNβ-1b (26). Antiviral activities of the individual IFNβ-1b samples were calculated by comparison of their anticytopathic effect (CPE) with that of the NIBSC interferon beta Ser17 mutein standard (code: 00/574).

Data Analysis and Curve Fitting

MATLAB software version 7.1 (Math Works Inc., MA, USA) was used to numerically determine constant rates of aggregation by fitting experimental data in Eqs. 1 and 3.

RESULTS AND DISCUSSION

The commercially formulated IFNβ-1b contains numbers of large aggregates (1). Understanding the mechanism of aggregation of IFNβ-1b would help in minimizing this phenomenon.

The unformulated IFNβ-1b samples used in this study were all fresh, containing a monomer form of IFNβ-1b protein as concluded in Fig. 1. Also, values of $OD_{360\ nm}$ ~0.01 and $OD_{280\ nm}/OD_{260\ nm}$ ~1.5 were obtained for unformulated samples of IFNβ-1b at time zero (Fig. 2). As depicted in Fig. 2, thermal incubation of the samples without SDS at 37°C resulted in an increase in $OD_{360\ nm}$ of ~1.35 and a decrease in $OD_{280\ nm}/OD_{260\ nm}$ of ~1.0. IFNβ-1b showed the lowest ratio of $OD_{280\ nm}/OD_{260\ nm}$ and the highest $OD_{360\ nm}$ after 150 h, most likely caused by absorption flattening due to extensive aggregation of the sample (23). Turbidity occurred during aggregation of IFNβ-1b monomer solution. After centrifugation, a phase separation with a cloudy white lower phase (sometimes called *opalescence*) (11) was observed. On the other hand, $OD_{360\ nm}$ and $OD_{280\ nm}/OD_{260\ nm}$ of samples containing 0.1% of SDS did not change significantly (Fig. 2). By adding 0.1% (*v*/*v*) of SDS to cloudy aggregate solutions, the turbidity disappeared in few seconds, and at 360 nm, no absorption was shown. As SDS reduces non-covalent hydrogen bonds and hydrophobic interactions, the aggregates formed by IFNβ-1b monomers are apparently of non-covalent type.

The size distributions of the IFNβ-1b measured by DLS are shown in Fig. 3. While protein solution sample consists of monomers with a Z_{ave} of 7 nm, after 7 days of incubation, the

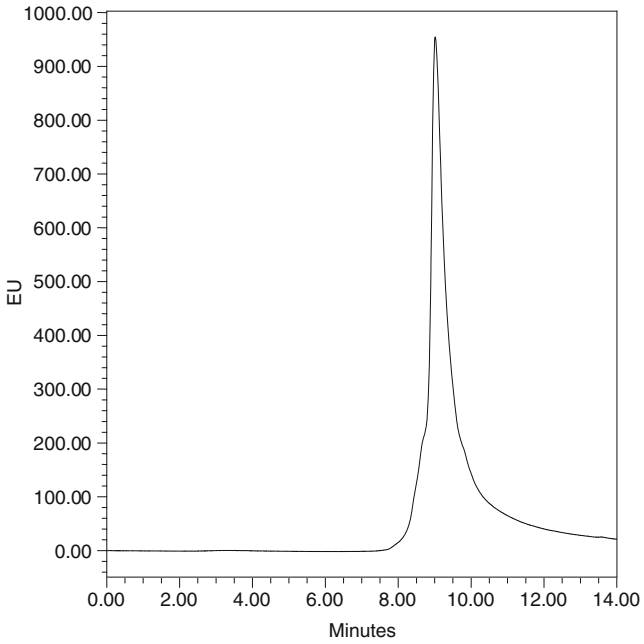

Fig. 1. The SEC chromatogram of fresh unformulated IFNβ-1b samples

size of proteins increased up to 85 nm, which indicates the tendency of the monomers for aggregation. Heterogeneity of IFNβ-1b increased during the first 3 days as detected by an increase in the PDI from 0.03 to 0.08. Protein aggregates in solution are usually heterogeneous; therefore, it is not easy to determine the exact size of the aggregates (27). However, after 3 days, most of the IFNβ-1b molecules were in the form of aggregates. The heterogeneity declined to 0.04 in the last days, and the aggregates mainly consisted of larger sizes.

Mechanism of Aggregation of IFNβ-1b

In this study, IFNβ-1b was treated with heat and H_2O_2 to determine aggregation rate parameters. During aggregation,

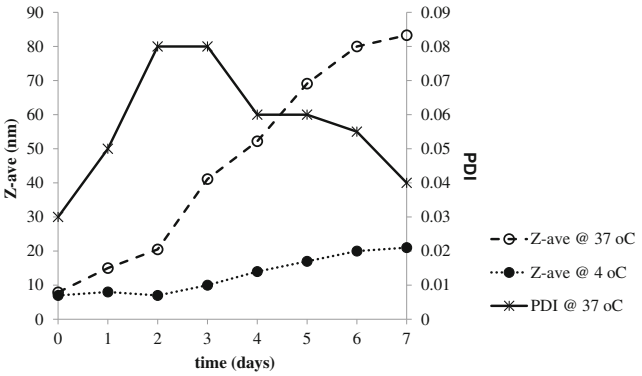

Fig. 3. The size distributions of the IFNβ-1b solution measured by dynamic light scattering (DLS), with two replicates

the monomer loss in solution was calculated at different time intervals. Supernatants were analyzed by DLS to be sure of aggregate-free solution (data not shown). The experimental kinetic data were fitted by an autocatalytic model to determine kinetic parameters (Table I).

We first explored the influence of heating on IFNβ-1b aggregation rates. Protein samples of 1.4 mg ml^{-1} were kept at 4, 25, 37, and 70°C for 10 days, and aggregation was analyzed twice a day. The DLS (Fig. 3) and monomer loss results (Fig. 4a) for the samples incubated at 4°C show that an unformulated monomer solution of IFNβ-1b could be kept in a refrigerator without any obvious aggregate formation up to 3 days. Obviously, for nucleus formation, more time is needed at 4°C, while at room temperature (25°C), aggregate formation occurs faster (Fig. 4a). On the other hand, heating at 37°C and 70°C increased the protein aggregation rate significantly. These data fit the autocatalytic model (Fig. 4a, solid lines) with a $R^2>0.99$ and $\chi^2<0.001$. These results suggest that a nucleation step in IFNβ-1b aggregation is likely (as it is understood from autocatalytic mechanism). Also, the lag time during incubation at 4°C is a sign for nucleus formation during aggregation of IFNβ-1b. It seems that heating increases the entropy of system and thereafter results in more changes in

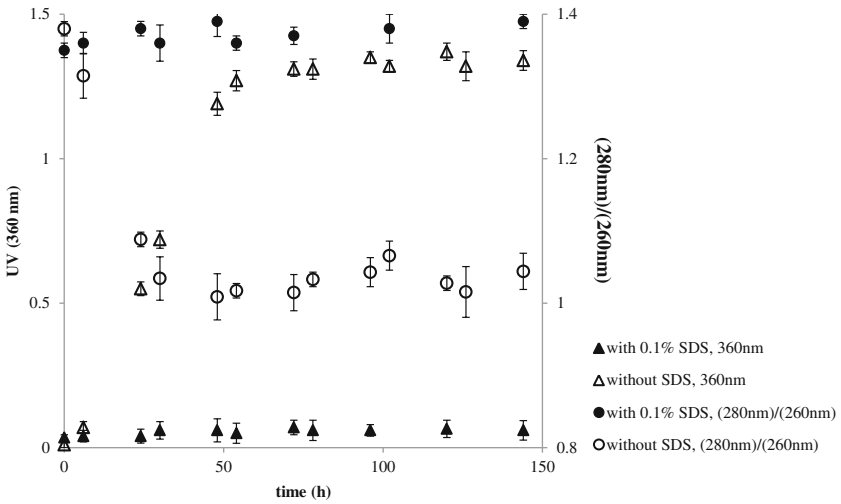

Fig. 2. Difference in UV intensity at 360 nm and the ratio of (280 nm)/(260 nm) between IFNβ-1b samples of uncovered or without SDS (*empty triangle* and *empty circle*) and SDS containing (*filled triangle* and *filled circle*) at 37°C, with two replicates

Table I. Nucleation (k_1) and Growth (k_2) Rate Constants of Aggregation of IFNβ-1b. Calculations by the Best Fit of Experimental Data to Eq. 1

Entry	Parameter	Value	k_1 (min^{-1})	k_2 (M^{-1} min^{-1})
1	Heating (°C)	4	$2.3\pm0.1\times10^{-6}$	$7.0\pm0.3\times10^{-9}$
		25	$1.5\pm0.2\times10^{-4}$	$2.9\pm0.2\times10^{-8}$
		37	$7.0\pm0.1\times10^{-4}$	$9.0\pm0.1\times10^{-9}$
		70	$6.0\pm0.1\times10^{-3}$	$2.4\pm0.4\times10^{-7}$
2	Oxidizing (% *v/v*)	0.0	$1.5\pm0.2\times10^{-4}$	$2.9\pm0.2\times10^{-8}$
		0.3	$2.8\pm0.3\times10^{-2}$	$2.7\pm0.5\times10^{-6}$
		0.6	$2.1\pm0.2\times10^{-1}$	$2.0\pm0.2\times10^{-5}$
		3.0	$1.0\pm0.1\times10^{0}$	$6.5\pm0.0\times10^{-5}$
3	IFNβ-1b concentration (mg/ml)	0.6	$1.6\pm0.3\times10^{-4}$	$1.1\pm0.1\times10^{-10}$
		1.0	$1.2\pm0.4\times10^{-4}$	$3.8\pm1.0\times10^{-9}$
		1.4	$2.0\pm0.1\times10^{-4}$	$9.0\pm0.1\times10^{-9}$
4	Seeding (% *w/w*)	0.0	$1.5\pm0.2\times10^{-6}$	$3.1\pm0.2\times10^{-8}$
		1.0	$5.2\pm0.2\times10^{-5}$	$1.7\pm0.3\times10^{-8}$
		3.0	$8.7\pm0.1\times10^{-5}$	$3.9\pm0.1\times10^{-8}$

Mean±SD, with two replicates

the conformation of IFNβ-1b and facilitates aggregate formation. Table I shows the estimated values for nucleation, and growth rate constants (k_1 and k_2) are presented.

We also explored the use of H_2O_2 as an inducer of aggregation of IFNβ-1b. The effect of 0.6, 0.3, and 3.0% *v/v* of H_2O_2 on unformulated IFNβ-1b was analyzed. Figure 4b shows the fitting of the experimental data on the autocatalytic model. After 5-min exposure to 3.0% *v/v* of H_2O_2 more than 90% of monomers vanished, indicating extensive aggregation. The experimental data for all ranges of H_2O_2 concentrations fitted the model, with $R^2 \geq 0.99$ and $\chi^2 \leq 0.001$. The effect of H_2O_2 on aggregation constant rates is depicted in Table I, entry 2. Results show that nucleation and growth rate constants of aggregation increased considerably by the presence of an oxidizing agent. H_2O_2 in a concentration of 3.0% *v/v* was able to increase k_1 from $1.5\pm0.2\times10^{-4}$ to $1.0\pm0.1\times10°min^{-1}$ and k_2 from $2.9\pm0.2\times10^{-8}$ to $6.5\pm0.0\times10^{-5}$ M^{-1} min^{-1}. Therefore, nucleation is a critical step in aggregation of IFNβ-1b and H_2O_2 facilitates this step. Oxidization-induced aggregation is fast and easy and could be as an alternative to heating in protein aggregation studies.

The reaction pathways of autocatalytic model consist of irreversible formation of aggregates. Therefore, IFNβ-1b is supposed to follow an irreversible nucleus formation mechanism from single monomer protein during aggregation. This single-molecule nucleus can be compared with the aggregation-prone monomers as defined recently by Kayser *et al.* (28).

To study the effect of initial monomer concentration ($[M_0]$) on aggregation of IFNβ-1b, samples containing 0.6, 1.0, and 1.4 mg ml^{-1} of unformulated IFNβ-1b monomers were incubated at 37°C. Experimental data collected during 200 h of incubation were fitted using an autocatalytic model as shown in Fig. 4c, indicating good fitting with $R^2 \geq 0.99$ and $\chi^2 \leq 0.001$. Rate constants of nucleation (k_1) and growth (k_2) for IFNβ-1b estimated at different concentrations of initial monomer are presented in Table I, entry 3. The nucleation rates of aggregation slightly changed by increasing the concentration of monomers from 0.6 to 1.4 mg ml^{-1}. Therefore, the accumulation of

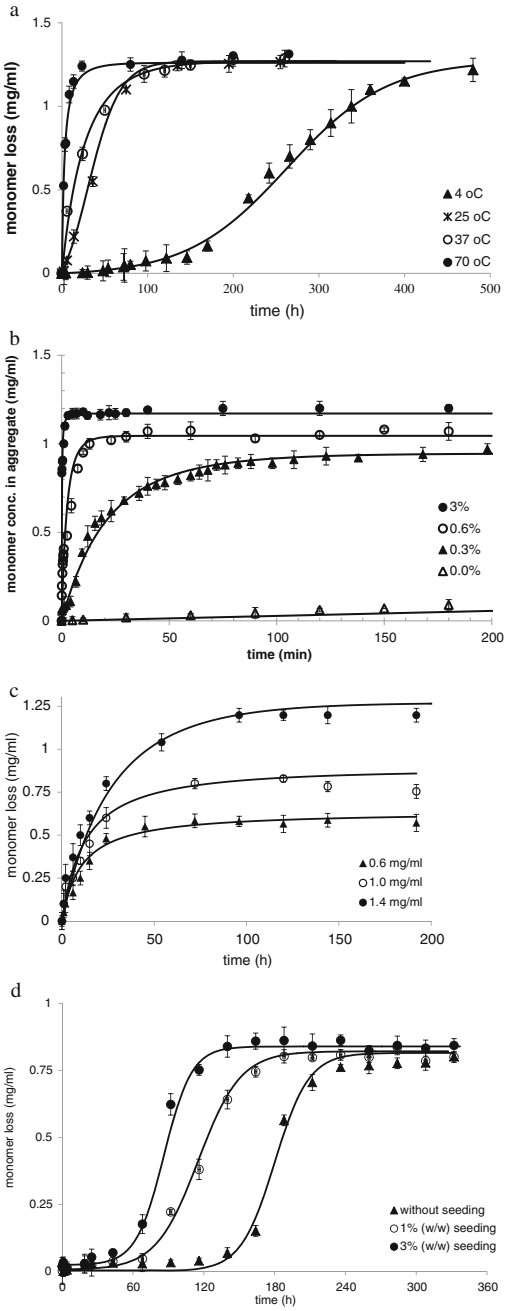

Fig. 4. Effect of temperature, oxidation, monomer initial concentration, and seeding on aggregation rate of IFNβ-1b. *Lines* are the best fit of experimental data to autocatalytic model given by Eq. 1. The experiments were performed in two replicates ($n=2$). **a** Effect of temperature on aggregation rate of IFNβ-1b. Data were collected at different temperatures of 4°C (*filled triangle*), 25°C (*multiplication sign*), 37°C (*filled circle*), and 70°C (*empty circle*). $\chi^2<0.001$ and $R^2>0.99$. **b** Effect of H_2O_2 concentration on aggregation of IFNβ-1b. Data were collected at different H_2O_2 concentrations of 0.3% *v/v* (*filled triangle*), 0.6% *v/v* (*empty circle*), 3.0% *v/v* (*filled circle*), and 0.0% *v/v* (*empty triangle*). $\chi^2<0.001$ and $R^2>0.99$. **c** Effect of concentration of IFNβ-1b monomer solution on aggregation rate at 37°C. Data were collected at different IFNβ-1b concentrations of 0.6 mg ml^{-1} (*filled triangle*), 1.0 mg ml^{-1} (*empty circle*), and 1.4 mg ml^{-1} (*filled circle*). $\chi^2<0.001$ and $R^2>0.99$. **d** Effect of seeding on aggregation rate. Data were collected at different concentrations of seed: without seed (*filled triangle*), 1% (*w/w*) (*empty circle*), and 3% (*w/w*) (*filled circle*). $\chi^2<0.001$ and $R^2>0.99$

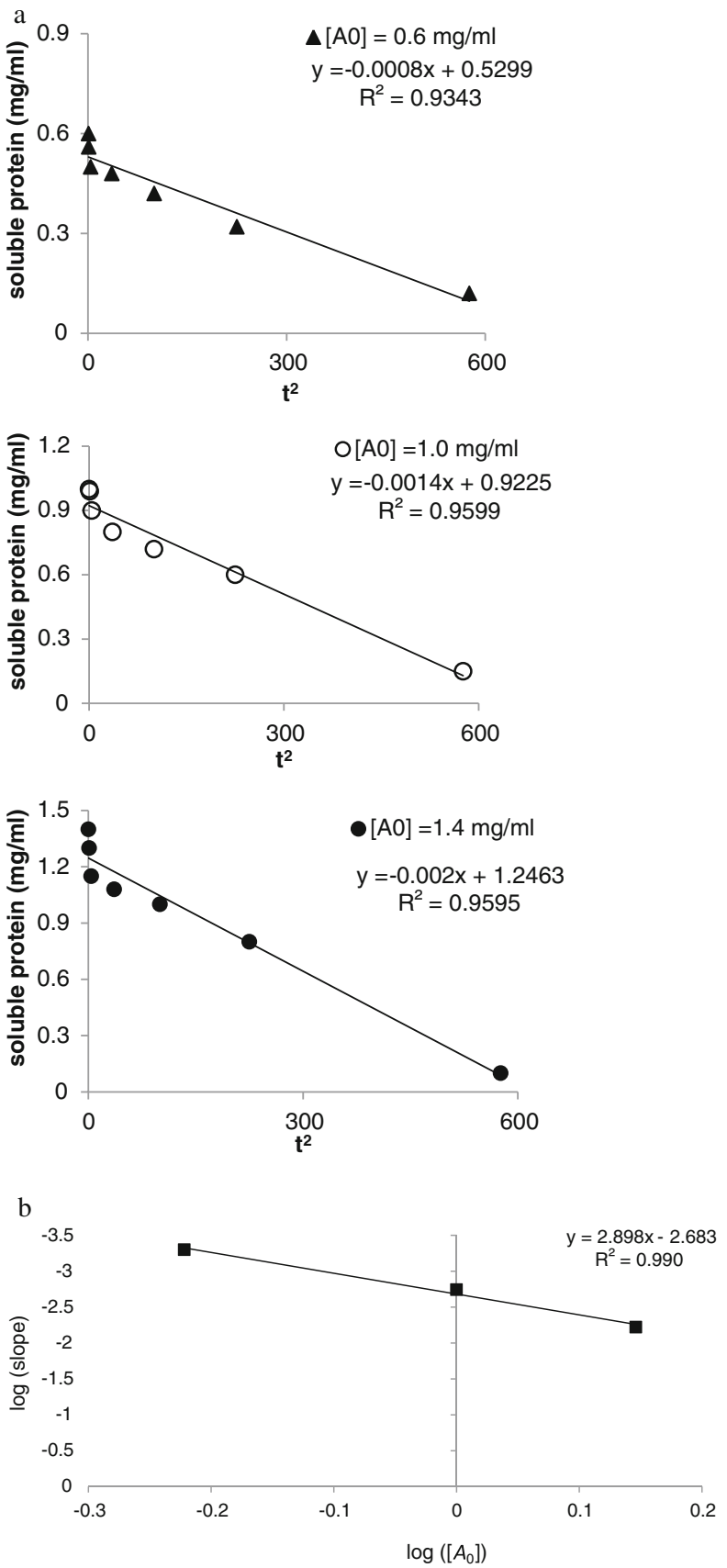

Fig. 5. The approach of Chen *et al.* estimating the number of monomers in the nucleus of aggregation (24). **a** t^2 plot of IFNβ-1b at 0.6, 1.0, and 1.4 mg ml^{-1} of unformulated IFNβ-1b monomers. **b** Linear fit of log(α) *vs.* log([A_0])

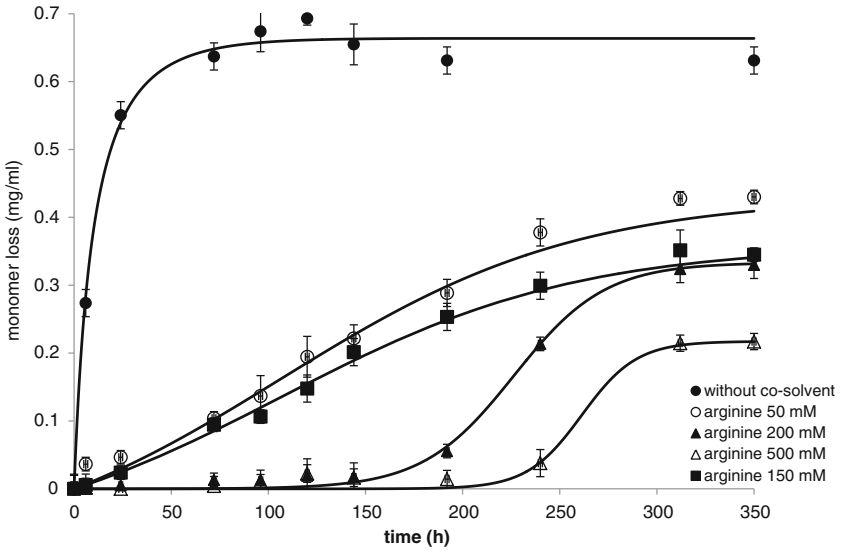

Fig. 6. Anti-aggregation effect of different concentrations of arginine on aggregation of IFNβ-1b. *Lines* are the best fit of experimental data to autocatalytic model given by Eq. 1

monomeric IFNβ-1b molecules and initial monomer concentration could not be the main cause of aggregation, at least at the range which was tested in this study. Probably, the nucleus is a single monomer molecule with potential to growing higher molecular weight aggregates. These results were confirmed by the approach of Chen *et al.*, estimating the number of monomers in the nucleus of aggregation (24). Only data of the first 24 h were used to estimate n^*, because of the high validity of the data obtained at early aggregation steps (Fig. 5). Figure 5a shows t^2 plot of IFNβ-1b at 0.6, 1.0, and 1.4 mg ml^{-1} of unformulated IFNβ-1b monomers, and Fig. 5b is the linear fit of log(α) *vs.* log([A_0]). We obtained a value of $n^*=0.9$ and $k'=6.0\times10^{-10}$ M^{-2} min^{-2} with $R^2>0.99$. This confirms that in protein concentrations of <1.4 mg ml^{-1}, a single-molecule nucleus is formed as a primary step in the aggregation step of IFNβ-1b. Consequently, the nucleus is a monomer which has been modified or deformed from its native conformation.

The effect of seeding of monomer solution with aggregate proteins was studied by calculation kinetic rates of aggregation. A 1.4 mg ml^{-1} IFNβ-1b solution containing more than 95% soluble aggregate was used as seed. Seeding was performed by adding 1.0% (*w*/*w*) and 3.0% (*w*/*w*) of the aggregate sample to the monomer-containing samples of IFNβ-1b solution with a concentration of 1.4 mg ml^{-1}. Samples were incubated at 4°C for 10 days, and the monomer loss was calculated. Data were fit by Eq. 1 ($R^2>97\%$ and $\chi^2<0.01$) to calculate nucleation (k_1) and growth (k_2) rate constants of aggregation (Fig. 4d). Results show that the seeding had a considerable effect on IFNβ-1b nucleation rate of aggregation (k_1), whereas a mild change in growth rate of aggregation was observed. The nucleation rate of aggregation (k_1) was increased from $1.5\pm0.2\times10^{-6}$ to $4.2\pm0.2\times10^{-5}$ min^{-1} and $8.7\pm0.1\times10^{-5}$ min^{-1} in samples seeded by 1.0% *w*/*w* and 3.0% *w*/*w* of pre-aggregated proteins, respectively (Table I, entry 4). The protein reached the nucleation step rapidly when aggregate seed was presented in solution. So, nucleation is a vital and rate-limiting step in launching the aggregation of IFNβ-1b. A minor difference was detected between nucleation constant rates (k_1) of 1.0% *w*/*w* and 3.0% *w*/*w*. Thus, the aggregation growth step initiates when up to 1.0% (*w*/*w*) of monomers are in nucleus form. This amount can be probably the critical concentration level of monomers in nucleus form to initiate large aggregate formation.

Anti-aggregation Effect of Arginine

IFNβ-1b samples of 1.4 mg ml^{-1} containing different concentrations of arginine (50, 200, and 500 mM) were incubated at room temperature. Aggregate formation of each sample was monitored precisely by reading OD at 360 nm (Fig. 6). Figure 6 shows that arginine concentrations higher than 200 mM are able to suppress aggregate formation in IFNβ-1b solutions of 1.4 mg ml^{-1}. The autocatalytic model was used to fit and determine nucleation rate constants for each sample with $R^2\geq0.99$ and $\chi^2\leq0.001$ (Table II). These results tend to suggest that arginine is able to suppress aggregate formation in IFNβ-1b solution by postponing the nucleation step which is demonstrated by a decrease in k_1. In the presence of 200 mM arginine, the nucleation rate constant of IFNβ-1b was significantly reduced from $3.9\pm1.1\times10^{-4}$ to $5.2\pm0.4\times10^{-6}$ min^{-1}, while a slight difference was obtained when the concentration was raised to 500 mM.

Table II. Nucleation (k_1) and Growth (k_2) Rate Constants of Aggregation of IFNβ-1b in the Presence of Different Concentrations of Arginine. Calculations by the Best Fit of Experimental Data to Eq. 1. $R^2>0.98$ and $\chi^2<0.0005$

	k_1 (min^{-1})	k_2 (M^{-1} min^{-1})
Control	$3.9\pm1.1\times10^{-4}$	$2.4\pm0.6\times10^{-7}$
Arginine 50 mM	$1.2\pm0.2\times10^{-5}$	$7.8\pm0.4\times10^{-7}$
Arginine 150 mM	$1.0\pm0.1\times10^{-5}$	$8.0\pm0.2\times10^{-7}$
Arginine 200 mM	$5.2\pm0.4\times10^{-6}$	$4.8\pm0.5\times10^{-7}$
Arginine 500 mM	$3.6\pm0.3\times10^{-6}$	$5.0\pm0.4\times10^{-7}$

Mean±SD, with two replicates

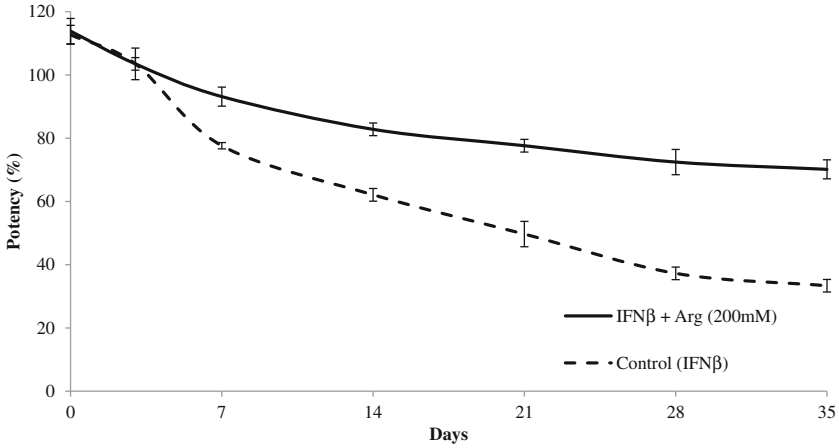

Fig. 7. Antiviral activity (potency) of IFNβ-1b in shelf life; unformulated samples as control (*dashed line*) and formulated by 200 mM of arginine (*solid line*)

Effect of Arginine on Antiviral Activity

The biological activity of IFNβ-1b solutions formulated by 200 mM arginine was evaluated. Samples of IFNβ-1b with and without arginine were incubated at room temperature for more than a month to assess the effect of 200 mM of arginine. A significant loss in activity was observed after 4 days in samples without arginine (Fig. 7). While a 35% decrease in activity was observed in samples containing arginine compared to 65% decrease in those lacking the amino acid additive, a concentration of 200 mM of arginine had a positive effect on the potency of IFNβ-1b after a month (Fig. 7).

ROS Detection

The considerable differences between kinetic rates of aggregation by oxidation and by increased temperature indicate that oxidation may be the main cause of IFNβ-1b aggregation. Thus, we tried to detect ROS during aggregation of IFNβ-1b solutions. Chemiluminescence was used to determine ROS such as the superoxide anion (O_2^-), H_2O_2, and the hydroxyl radical ($OH\cdot$) in heated IFNβ-1b. Monomer solutions were kept at 4, 25, and 70°C during different time periods of 2, 5, 10, 20, and 120 min and also for 10 days. While more than 99% of monomer proteins converted to aggregates after 10 min of incubation at 70°C, at temperatures of 4°C and 25°C, more time was required due to lower kinetic of aggregation as discussed (Fig. 4a); 3.0 μM of hydrogen peroxide was detected early (<5 min) in the samples heated at 70°C. Nothing was detected in samples incubated at 4°C and 25°C. Apparently, ROS can only be detected if protein aggregation is fast.

The question remains in what stage ROS is generated, during nucleation or growth steps. The presence of ROS seems to be limited to a period of 5–10 min after a sample is heated to a high temperature, indicating that these are generated during early nucleation and not the aggregation growth step. Due to the fast rate of the nucleation step, any effort to find ROS before or during this step was unsuccessful. Therefore, there is no evidence whether ROS will be generated during the shelf life of the protein solution at room temperature. We also failed to find the reason for generation of ROS during aggregation of IFNβ-1b.

Reversed phase (RP) HPLC was used to distinguish the oxidized form of IFNβ-1b from the native one. Figure 8a, b shows the chromatograms of the untreated samples and the samples treated with 3.0% *v*/*v* of H_2O_2, respectively. The retentions for native and oxidized form of IFNβ-1b were 26 and 25 min, correspondingly. In order to detect the oxidized form of protein in aggregates, monomer solutions of IFNβ-1b were incubated at 70°C for 10 min. Compared to monomer solutions, about 1% of total proteins were oxidized in the aggregate samples (Fig. 8c). Although the amount of oxidized protein is small, it may be sufficient to initiate aggregation. This quantity is consistent with those observed by the seeding method, showing the initiation of aggregation by a change in few monomers. So, it seems that oxidation could be the main cause of IFNβ-1b aggregation.

Also, the generation of ROS in IFNβ-1b monomer samples incubated at 70°C was studied for samples containing 200 mM of arginine. The chemiluminescence and RP HPLC results showed that by presenting arginine in IFNβ-1b solution, the ROS formation and oxidized form of protein are suppressed (data not shown). Therefore, ROS is generated if only aggregation is happening.

Previously, Chi *et al.* have proposed an irreversible stage of pre-nucleus formation for a protein system undergoing nucleation-dependent assembly, although they mention there are no published data showing aggregation of therapeutic proteins by this pathway (9). Also, Roberts and Li have suggested a reversible association of reactive monomers as pre-nucleation stage of aggregation of proteins (29).

ROS are generated under numerous conditions *in vivo* and have the ability, either directly or indirectly, to damage all biomolecules, including proteins. Oxidation of proteins by ROS can lead to inhibition of activities of proteins, altered immunogenicity, and increased susceptibility to aggregation (7).

Protein conformational stability may help to limit *protein* oxidation (30). However, once oxidation occurs, more destabilization of therapeutic protein structure happens which results in more conformational changes and decreases in stability (30,31). The tertiary structure of oxidized proteins is thermodynamically unstable, and therefore, oxidized proteins tend to expose hydrophobic amino acids to the outside environment which may lead to monomer association. Therefore,

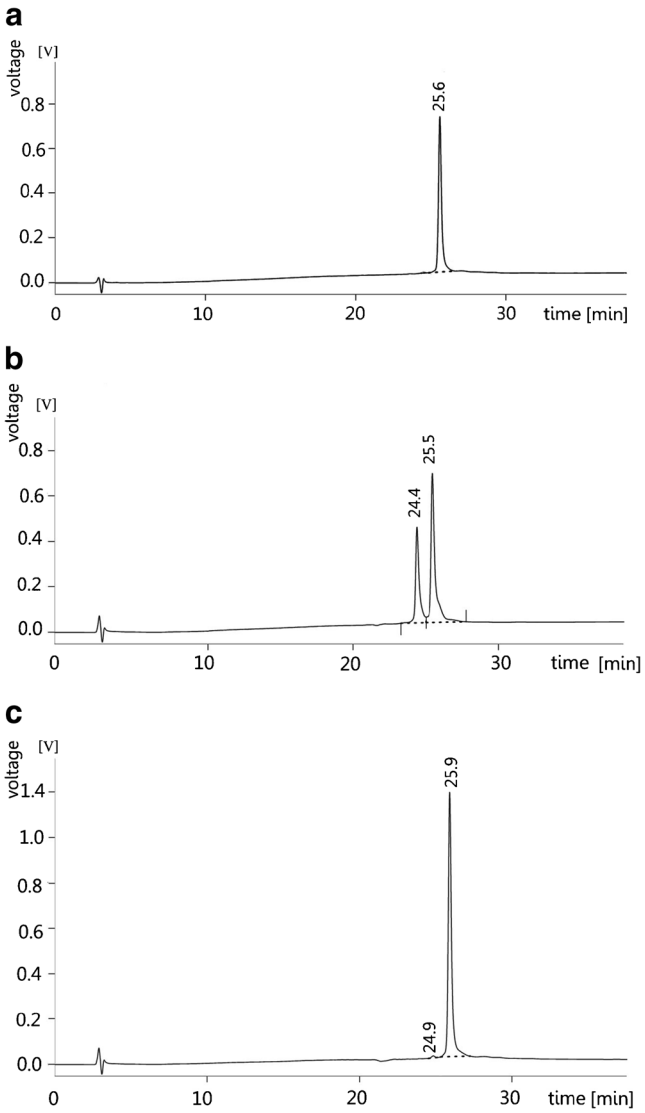

Fig. 8. RP HPLC chromatograms. **a** Non-induced IFNβ-1b solution. **b** Oxidation-induced IFNβ-1b by 3.0% *v/v* H_2O_2. **c** Thermally induced IFNβ-1b at 70°C

it is highly likely that oxidized molecule species form a pre-nucleus during initial stages of aggregation. Consequently, IFNβ-1b-oxidized monomers form the pre-nuclei which force aggregation by speeding up the nucleation step in solution. By reaching a critical concentration level in pre-nucleus step (1% of total protein content), nucleation step starts promptly.

We propose the new pre-nucleus model in order to improve the autocatalytic model for protein systems undergoing pre-nucleation and chemical modifications in monomers (e.g., oxidation) prior to aggregate formation. Therefore, irreversible modification of minor monomers (M) results in pre-nucleus (N^*) formation. It is supposed that pre-nucleus species are energetically unstable, and eventually, they deform to nuclei (N). The nucleus is in equilibrium with pre-nucleus species which is assumed to have different conformations. This nucleus can also be defined as aggregation-prone monomers as defined by Kayser *et al.* (28). Nucleus (N) converts to aggregates of A by binding to free monomers, irreversibly. Afterwards, aggregates start to grow by binding to other free monomers. The following scheme describes these pathways:

$$M \xrightarrow{k^*} N^* \underset{k_{-n}}{\overset{k_n}{\rightleftarrows}} N$$
$$M + N \xrightarrow{k_1} A$$
$$M + A \xrightarrow{k_2} A$$

where k^* is the pre-nucleation rate constant and k_n and k_{-n} are the rate constants of equilibration between N and N^*. By assuming a quasi-steady state, the intermediate nucleus reacts as quickly as it forms. Therefore, equations will be

$$\begin{cases} \dfrac{-1}{[M]}\dfrac{d[M]}{d[t]} = k^* + k([M_0]-[M]-[A]) + k_2[A] \\ \dfrac{1}{[M]}\dfrac{d[A]}{d[t]} = k([M_0]-[M]-[A]) \end{cases} \tag{3}$$

Table III. Rate Constants of Aggregation of IFNβ-1b (1) at Different Inducing Temperatures and (2) in the Presence of Different Concentrations of Arginine; Calculations by the Best Fit of Experimental Data to Pre-nucleus Model Equation. $R^2>0.99$ and $\chi^2<0.0001$

Entry		$k^*(\text{min}^{-1})$	k_n (M^{-1} min^{-1})	k_{-n} (M^{-1} min^{-1})	k_1 (M^{-1} min^{-1})	k_2 (M^{-1} min^{-1})
1	4	$7.5\pm0.4\times10^{-5}$	$1.7\pm0.8\times10^{-8}$	$3.5\pm0.3\times10^{-8}$	$2.3\pm1.1\times10^{-9}$	$2.5\pm0.7\times10^{-8}$
	25	$3.5\pm0.2\times10^{-3}$	$9.8\pm1.9\times10^{-7}$	$8.8\pm0.1\times10^{-7}$	$9.3\pm0.7\times10^{-8}$	$7.7\pm0.9\times10^{-8}$
	37	$5.4\pm0.1\times10^{-2}$	$7.5\pm0.4\times10^{-7}$	$4.1\pm0.1\times10^{-7}$	$7.7\pm0.8\times10^{-8}$	$7.5\pm0.4\times10^{-8}$
	70	$1.1\pm0.0\times10^{-1}$	$2.3\pm0.6\times10^{-7}$	$1.1\pm0.0\times10^{-7}$	$2.7\pm0.2\times10^{-7}$	$7.7\pm0.5\times10^{-7}$
2	Control	$8.8\pm0.1\times10^{-4}$	$7.5\pm1.0\times10^{-6}$	$2.1\pm1.1\times10^{-6}$	$3.9\pm0.5\times10^{-8}$	$3.5\pm0.8\times10^{-8}$
	Arginine 50 mM	$1.8\pm0.3\times10^{-5}$	$7.0\pm0.9\times10^{-7}$	$8.1\pm0.5\times10^{-7}$	$3.5\pm0.7\times10^{-8}$	$1.1\pm1.0\times10^{-8}$
	Arginine 200 mM	$5.3\pm0.7\times10^{-7}$	$1.1\pm0.9\times10^{-7}$	$2.1\pm1.4\times10^{-7}$	$2.0\pm0.5\times10^{-8}$	$3.5\pm1.1\times10^{-8}$
	Arginine 500 mM	$4.3\pm0.5\times10^{-7}$	$1.0\pm0.8\times10^{-7}$	$1.2\pm0.8\times10^{-7}$	$3.5\pm0.9\times10^{-8}$	$2.9\pm0.7\times10^{-8}$

Mean±SD, with two replicates

where

$$k = k_1/\left(1+\frac{k_{-n}+k_1[M]}{k_n}\right)$$

The pre-nucleus model was used to study the rate of aggregation of IFNβ-1b and the anti-aggregation effect of arginine. Data obtained by thermal heating of samples were fitted by pre-nucleus model equation (Eq. 3). Table III shows the rate constants obtained using pre-nucleus model. These results tend to suggest that by increasing temperature, a significant increase in pre-nucleus rate constant (k^*) of aggregation of unformulated IFNβ-1b is obtained (Table III, entry 1). On the other hand, milder change was obtained for rate constants of equilibration and aggregation growth. These results prove the tendency of IFNβ-1b molecules in pre-nucleus formation prior to nucleus and higher molecular weight aggregate formation.

By increasing arginine concentration in protein solution, considerable decrease in pre-nucleus rate constant was observed (Table III, entry 2). Arginine with a concentration of 200 mM was able to reduce a constant rate of pre-nucleation from $8.8\pm0.1\times10^{-4}$ to $5.3\pm0.7\times10^{-7}$ min^{-1}. Therefore, arginine suppresses aggregate formation by controlling pre-nucleus formation during aggregation of IFNβ-1b.

CONCLUSION

Mechanism of aggregation of IFNβ-1b was determined in this study. A pre-nucleation rate-limiting step controls the kinetic of aggregation of IFNβ-1b. ROS (e.g., H_2O_2) were generated in early stages of aggregation of IFNβ-1b. Oxidized monomers of IFNβ-1b are presented as unstable pre-nucleus structures which are prone to nonnative aggregation by conformational changes. The pre-nucleus model was presented for IFNβ-1b and probably other proteins undergoing chemical modifications during aggregation. We showed that arginine with a concentration of 200 mM was able to slow down IFNβ-1b aggregation considerably and has a progressive effect on its biological activity. These influences probably arise from the decreasing effect of arginine on the rate of pre-nucleation during aggregate formation. We believe that arginine could be used as a cosolvent in formulation of IFNβ-1b in the future. This will be more investigated in our upcoming research. Also, it would be desirable to gather direct evidence of the effect of ROS generation on protein aggregation. This appears to be a rewarding future project.

REFERENCES

1. Barnard JG, Babcock K, Carpenter JF. Characterization and quantitation of aggregates and particles in interferon-β products: potential links between product quality attributes and immunogenicity. J Pharm Sci. 2013;102:915–28.
2. Hermeling S, Jiskoot W, Crommelin D, Bornæs C, Schellekens H. Development of a transgenic mouse model immune tolerant for human interferon beta. Pharm Res. 2005;22:847–51.
3. Runkel L, Meier W, Pepinsky RB, Karpusas M, Whitty A, Kimball K, *et al*. Structural and functional differences between glycosylated and non-glycosylated forms of human interferon-beta (IFN-beta). Pharm Res. 1998;15:641–9.
4. van Beers MMC, Sauerborn M, Gilli F, Brinks V, Schellekens H, Jiskoot W. Aggregated recombinant human interferon beta induces antibodies but no memory in immune-tolerant transgenic mice. Pharm Res. 2010;27:1812–4.
5. van Beers MMC, Sauerborn M, Gilli F, Brinks V, Schellekens H, Jiskoot W. Oxidized and aggregated recombinant human interferon beta is immunogenic in human interferon beta transgenic mice. Pharm Res. 2011;28:2393–402.
6. Luo Q, Joubert MK, Stevenson R, Ketchem RR, Narhi LO, Wypych J. Chemical modifications in therapeutic protein aggregates generated under different stress conditions. J Biol Chem. 2011;286:25134–44.
7. Shater E. Qualification and significance of protein oxidation in biological samples. Drug Metab Rev. 2000;32:307–26.
8. Mirzaei H, Regnier F. Protein: protein aggregation induced by protein oxidation. J Chromatogr B Anal Technol Biomed Life Sci. 2008;873:8–14.
9. Chi EY, Krishnan S, Randolph TW, Carpenter JF. Physical stability of proteins in aqueous solution: mechanism and driving forces in nonnative protein aggregation. Pharm Res. 2003;20:1325–36.
10. Andrews JM, Roberts CJ. A Lumry-Eyring nucleated polymerization model of protein aggregation kinetics: 1. Aggregation with pre-equilibrated unfolding. J Phys Chem B. 2007;111:7897–913.
11. Mahler HC, Friess W, Grauschopf U, Kiese S. Protein aggregation: pathways, induction factors and analysis. J Pharm Sci. 2009;98:2909–34.
12. Arakawa T, Tsumoto K, Kita Y, Chang B, Ejima D. Biotechnology application of amino acids in protein purification and formulation. Amino Acids. 2007;33:587–605.
13. Arakawa T, Ejima D, Tsumoto K, Obeyama N, Tanaka Y, Kita Y, *et al*. Suppression of protein interactions by arginine: a proposed mechanism of the arginine effects. Biophys Chem. 2007;127:1–8.
14. Lange C, Rudolph R. Suppression of protein aggregation by L-arginine. Curr Pharm Biotechnol. 2009;10:408–14.

15. Tsumoto K, Umetsu M, Kumagai I, Philo JS, Arakawa T. Role of arginine in protein refolding, solubilization, and purification. Biotechnol Prog. 2004;20:1301–18.
16. Nakakido M, Kudou M, Arakawa T, Tsumoto K. To be excluded or to bind, that is the question: arginine effects on proteins. Curr Pharm Biotechnol. 2009;10:415–20.
17. Shukla D, Trout BL. Interaction of arginine with proteins and the mechanism by which it inhibits aggregation. J Phys Chem B. 2010;114:13426–38.
18. Baynes BM, Trout BL. Rational design of solution additives for the prevention of protein aggregation. Biophys J. 2004;87:1631–9.
19. Morris AM, Watzky MA, Finke RG. Protein aggregation mechanism, and curve-fitting: a review of the literature. Biochim Biophys Acta. 2009;1794:375–97.
20. Bernacki JP, Murphy RM. Model discrimination and mechanistic interpretation of kinetic data in protein aggregation studies. Biophys J. 2009;96:2871–87.
21. Fazeli A, Shojaosadati SA, Fazeli MR, Ilka H. Effect of parallel feeding of oxidizing agent and protein on fed-batch refolding process of recombinant IFNβ-1b. Process Biochem. 2011;46:796–800.
22. Primm TP, Walker KW, Gilbert HF. Facilitated protein aggregation. Effects of calcium on the chaperone and anti-chaperone activity of protein disulfide-isomerase. J Biol Chem. 1996;271:33664–9.
23. Kueltzo LA, Middaugh CR. Ultraviolet absorption spectroscopy. In: Jiskoot W, Crommelin DJA, editors. Methods for structural analysis of protein pharmaceuticals, vol. III. Arlington: AAPS; 2007.
24. Chen S, Ferrone FA, Wetzel R. Huntington's disease age-of-onset linked to polyglutamine aggregation nucleation. Proc Natl Acad Sci U S A. 2002;99:11884–9.
25. Shourian M, Tavakoli H, Ghourchian H, Rafiee-Pour HA. Detection and dosimetry of gamma ray emitted from thallium-201 and technetium-99m based on chemiluminescence technique. Radiat Meas. 2010;45:906–10.
26. Lallemand C, Meritet JF, Erickson R, Grossberg SE, Roullet E, Lyon-Caen O, *et al.* Quantification of neutralizing antibodies to human type I interferons using division-arrested frozen cells carrying an interferon-regulated reporter-gene. J Interferon Cytokine Res. 2008;28:393–404.
27. Filipe V, Hawe A, Jiskoot W. Critical evaluation of nanoparticle tracking analysis (NTA) by NanoSight for the measurement of nanoparticles and protein aggregates. Pharm Res. 2010;27:796–810.
28. Kayser V, Chennamsetty N, Voynov V, Helk B, Forrer K, Trout BL. Evaluation of a non-Arrhenius model for therapeuti c monoclonal antibody aggregation. J Pharm Sci. 2011;100:2526–42.
29. Roberts CJ, Li Y. A Lumry-Eyring nucleated-polymerization (LENP) model of protein aggregation kinetics. 2. Competing growth via condensation and chain polymerization. J Phys Chem B. 2009;113:7020–32.
30. Thirumangalathu R, Krishnan S, Bondarenko P, Speed-Ricci M, Randolph TW, Carpenter JF, *et al.* Oxidation of methionine residues in recombinant human interleukin-1 receptor antagonist: implications of conformational stability on protein oxidation kinetics. Biochemistry. 2007;46:6213–24.
31. Bobst CE, Thomas JJ, Salinas PA, Savickas P, Kaltashov IA. Impact of oxidation on protein therapeutics: conformational dynamics of intact and oxidized acid-β-glucocerebrosidase at near-physiological pH. Protein Sci. 2010;19:2366–78.